Published in final edited form as:
Gene Ther. 2007 February ; 14(3): 219–226.

Glucose-6-phosphate transporter gene therapy corrects metabolic and myeloid abnormalities in glycogen storage disease type Ib mice

Wai Han Yiu, **Chi-Jiunn Pan**, **Mohammad Allamarvdasht**, **So Youn Kim**, and **Janice Y. Chou***
Section on Cellular Differentiation, Heritable Disorders Branch, National Institute of Child Health and Human Development, National Institutes of Health, Bethesda, MD 20892

Abstract

Glycogen storage disease type Ib (GSD-Ib) is caused by a deficiency in the glucose-6-phosphate transporter (G6PT), an endoplasmic reticulum-associated transmembrane protein that is ubiquitously expressed. GSD-Ib patients suffer from disturbed glucose homeostasis and myeloid dysfunctions. To evaluate the feasibility of gene replacement therapy for GSD-Ib, we have infused adenoviral (Ad) vector containing human G6PT (Ad-hG6PT) into G6PT-deficient ($G6PT^{-/-}$) mice that manifest symptoms characteristics of the human disorder. Ad-hG6PT-infusion restores significant levels of G6PT mRNA expression in the liver, bone marrow, and spleen and corrects metabolic as well as myeloid abnormalities in $G6PT^{-/-}$ mice. The $G6PT^{-/-}$ mice receiving gene therapy exhibit improved growth; normalized serum profiles for glucose, cholesterol, triglyceride, uric acid, and lactic acid; and reduced hepatic glycogen deposition. The therapy also corrects neutropenia and lowers the elevated serum levels of granulocyte colony stimulating factor. The development of bone and spleen in the infused $G6PT^{-/-}$ mice is improved and accompanied by increased cellularity and normalized myeloid progenitor cell frequencies in both tissues. This effective use of gene therapy to correct metabolic imbalances and myeloid dysfunctions in GSD-Ib mice holds promise for the future of gene therapy in humans.

Keywords

glycogen storage disease type Ib; adenoviral vector; gene therapy; glucose-6-phosphate transporter; bone marrow transduction; spleen transduction

Introduction

Glycogen storage disease type Ib (GSD-Ib) is an autosomal recessive disorder caused by a deficiency in the glucose-6-phosphate transporter (G6PT).[1,2] The primary function of G6PT, a ubiquitously expressed protein[3], is to translocate glucose-6-phosphate (G6P) from the cytoplasm of a cell to the lumen of the endoplasmic reticulum (ER) where it is hydrolyzed to glucose by glucose-6-phosphatase-α in the terminal steps of gluconeogenesis and glycogenolysis.[1,2] GSD-Ib patients manifest disturbed glucose homeostasis characterized by fasting hypoglycemia, hepatomegaly, nephromegaly, hyperlipidemia, hyperuricemia, lactic acidemia, and growth retardation.[1,2] In addition, GSD-Ib patients manifest neutropenia along with myeloid dysfunctions in Ca^{2+} mobilization, respiratory burst, and chemotaxis.[4-6] Since

*Corresponding author, Building 10, Room 9D42, NIH, 9000 Rockville Pike, Bethesda, MD 20892-1830, Tel: 301-496-1094; Fax: 301-402-6035, Email: chouja@mail.nih.gov

the primary gluconeogenic tissues are the liver and kidney, these additional symptoms suggest that myeloid tissues might be the most important non-gluconeogenic sites for G6PT expression.

The current treatment for GSD-Ib consists of a dietary therapy, including continuous nasogastric infusion of glucose[7] or frequent oral administration of uncooked cornstarch[8], to correct the loss of glucose homeostasis, augmented with granulocyte colony stimulating factor (G-CSF) therapy[9,10], to restore myeloid functions. The combined dietary and G-CSF therapies significantly alleviate the metabolic and myeloid abnormalities of GSD-Ib patients and greatly improve their prognosis. However, the underlying pathological process remains untreated and as a result, long-term complications, such as kidney disease in the form of renal calculi and progressive renal disease, inflammatory bowl disease, hepatic adenomas, and following G-CSF therapy, splenomegaly, develop in a significant percent of adult patients. Moreover, the efficacy of dietary treatment is frequently limited due to poor compliance.

G6PT is a hydrophobic protein anchored to the ER by ten-transmembrane helices.[11] While protein replacement therapy is not an option, somatic gene therapy, targeting the G6PT gene to the gluconeogenic and myeloid tissues is an attractive possibility. To develop novel therapies for GSD-Ib, we have previously generated G6PT-deficient ($G6PT^{-/-}$) mice that manifest all known metabolic and myeloid dysfunctions characteristics of the human disorder.[12] In addition to impaired glucose homeostasis, the $G6PT^{-/-}$ mice manifest neutropenia along with the increase in serum levels of G-CSF. The $G6PT^{-/-}$ mice exhibit impaired neutrophil respiratory burst activity as well as impaired chemotaxis and calcium flux. The bone and spleen of $G6PT^{-/-}$ mice are developmentally delayed and exhibit reduced cellularity, although the myeloid progenitor cell frequencies in bone marrow and spleen are increased.[12] In this study, we used the $G6PT^{-/-}$ mouse model to evaluate the feasibility of gene replacement therapy for GSD-Ib. We show that infusion of $G6PT^{-/-}$ mice with adenoviral (Ad) vector containing human G6PT (Ad-hG6PT) effectively delivers the G6PT transgene to the liver, bone marrows and spleen and markedly improves their survival. Ad-hG6PT-mediated gene transfer also corrects metabolic and myeloid abnormalities in GSD-Ib.

Results

Neonatal Ad-G6PT infusion directs G6PT expression in gluconeogenic and myeloid tissues

G6PT is a ubiquitously expressed gene but the expression levels of G6PT mRNA in gluconeogenic and myeloid tissues have not been measured quantitatively. Real-time PCR was used to measure the level of expression of the mouse G6PT gene in RNA isolated from liver, kidney, bone marrow, and spleen of wild-type mice and expressed relative to GAPDH RNA; the expression levels were then normalized by the level of G6PT transcript in the liver, which was arbitrarily defined as 100%. At 2 to 3 weeks of age, the levels of G6PT transcript in the kidney, bone marrow, and spleen were 51.8%, 7.8%, and 10.2%, of that in the mouse liver, respectively (Figure 1a).

Neonatal $G6PT^{-/-}$ mice were infused intravenously with 5×10^7 plaque forming units (PFU) of Ad-hG6PT and simultaneously, the glucose therapy was terminated. At 2 weeks post-infusion, hG6PT transcripts in the liver, kidney, bone marrow, and spleen in the infused animals were quantified using a human G6PT-specific probe that detects the transduced hG6PT but not the endogenous mouse G6PT transcripts (data not shown). The levels of hG6PT mRNA expression in kidney, bone marrow, and spleen were also normalized as described. Real-time PCR analysis shows that Ad-hG6PT efficiently delivered the transgene to the liver (100%), bone marrow (6.9%), and spleen (23.3%) but only a very low level of the transgene to the kidney (3.1%) (Figure 1b).

G6PT is an ER-associated transmembrane protein and appropriate membrane insertion is required for activity. G6PT$^{-/-}$ mice were analyzed for expression of recombinant G6PT by microsomal G6P uptake assays. In wild-type mice, postnatal microsomal G6P transport activity increased gradually to peak about age 4 weeks (Figure 1c), as was shown previously.[13] At 1 and 2 weeks post-Ad-hG6PT infusion, microsomal G6P transport activity in the liver reached 0.122 ± 0.017 and 0.130 ± 0.006 *nmol/mg/3 min*, respectively, representing 38% and 29% of the activities in hepatic microsomes of 1- and 2-week-old G6PT$^{+/+}$ mice, respectively (Figure 1c). Hepatic G6PT activity in the infused animals declined gradually and was only 1.3% of control levels at 4 weeks post-infusion. As expected, low or non-detectable levels of G6P uptake activity were observed in the kidney of the infused G6PT$^{-/-}$ mice at either 1 or 2 week post-infusion (data not shown).

Neonatal Ad-hG6PT-Infusion corrects metabolic abnormalities of GSD-Ib

G6PT$^{-/-}$ mice suffer from frequent hypoglycemic seizures and in the in the absence of any form of therapy most G6PT$^{-/-}$ mice die within the first two weeks of life.[12] Glucose homeostasis is maintained primarily by the hepatic G6Pase-α complex[1,2], thus delivery of a functional G6PT protein to the liver of G6PT$^{-/-}$ mice should restore their normal metabolic functions. Indeed, serum glucose profiles were normalized at 2 weeks post-infusion (Figure 2a) and none of the infused G6PT$^{-/-}$ mice suffered the frequent hypoglycemic seizures. There were no premature deaths of the Ad-hG6PT-infused G6PT$^{-/-}$ mice and their 4-week survival rate reached 100%. The G6PT$^{-/-}$ mice also manifest hypercholesterolemia, hypertriglyceridemia, hyperuricemia, and lactic acidemia (Figure 2a). At 2 weeks post-Ad-hG6PT infusion, there was a marked lowering in serum cholesterol, triglyceride, uric acid, and lactic acid profiles (Figure 2a).

G6PT$^{-/-}$ mice under glucose therapy are growth retarded[12] and by 2 weeks of age their average body weight is approximately 61% of their control littermates (Figure 2b). Ad-hG6PT infusion improved the growth of G6PT$^{-/-}$ mice and the average body weight of 2-week-old infused G6PT$^{-/-}$ mice was 83% of the G6PT$^{+/+}$ littermates (Figure 2b).

Hepatomegaly is another clinical presentation in GSD-Ib, which results from excessive glycogen accumulation in the liver.[1,2] Hematoxylin and eosin (H&E) staining revealed increased glycogen deposition in hepatocytes of G6PT$^{-/-}$ mice (Figure 3) and the average liver weight of 2 week-old G6PT$^{-/-}$ mice was elevated to 12.7% of body weight, compared to the wild-type value of 4.0% (Figure 2c). Ad-hG6PT infusion reduced hepatic glycogen storage in G6PT$^{-/-}$ mice (Figure 3) and the average liver weight in 2-week-old infused G6PT$^{-/-}$ mice reduced to 5.2 % of body weight (Figure 2c).

Nephromegaly is yet another clinical manifestation of human[1,2] and mouse[12] GSD-Ib. Since Ad-hG6PT infusion failed to deliver a significant levels of the G6PT transgene to the kidney, nephromegaly (Figure 2c) as well as renal glycogen storage (Figure 3) were not improved by Ad-hG6PT infusion.

Neonatal Ad-hG6PT-Infusion corrects myeloid dysfunctions of GSD-Ib

Neutropenia is a clinical characteristic of GSD-Ib patients[1,2] and mice.[12] Differential peripheral blood leukocyte counts revealed that neutrophil counts in 2-week-old G6PT$^{-/-}$ mice only average 19% of the counts in the G6PT$^{+/+}$ littermates (Figure 4a). Ad-hG6PT infusion improved neutropenia manifested by G6PT$^{-/-}$ mice and neutrophil counts increased to 52% of the counts in the control animals (Figure 4a).

In G6PT$^{-/-}$ mice, plasma G-CSF levels were abnormally increased, suggesting an underlying problem with neutrophil production.[12] Serum G-CSF values in 2-week-old G6PT$^{-/-}$ mice were 65-fold higher than those in the G6PT$^{+/+}$ littermates (Figure 4b). Ad-hG6PT infusion

normalized plasma cytokine levels and the levels of G-CSF in 2-week-old infused G6PT$^{-/-}$ mice were only 5-fold higher than those in the control animals (Figure 4b).

After birth, bone marrow is the primary origin and site of maturation and development of hematopoietic cells.[14] In neonatal mice, the spleen is also a hematopoietic organ.[15] In G6PT$^{-/-}$ mice, both bone and spleen were developmentally delayed.[12] Examination of femoral and tibia bones in 2-week-old G6PT$^{-/-}$ mice revealed that the epiphyses and growth plate were not well formed in contrast to those in the age-matched G6PT$^{+/+}$ littermates (Figure 5). While the white pulps in the spleen of 2-week-old G6PT$^{+/+}$ mice were clearly defined, the white pulps in the age-matched G6PT$^{-/-}$ spleen were not identifiable (Figure 5). Ad-hG6PT-infusion improved the development of bone and spleen, resulting in readily identifiable epiphyses and growth plates in the bone, and white pulps in the spleen, of 2-week-old infused G6PT$^{-/-}$ mice (Figure 5).

During the first 3 weeks of post-natal development, the medullary cavities of the femoral and tibia bones are disproportionately narrower and hypocellular in the G6PT$^{-/-}$ mice compared to controls.[12] Likewise, the spleens of G6PT$^{-/-}$ mice were disproportionably smaller than the age-matched control littermates.[12] The total numbers of cells in bone marrow aspirates combined from the femur and tibia in 2-week-old G6PT$^{-/-}$ mice were 17% of those in their age-matched G6PT$^{+/+}$ mice (Figure 6a). Ad-hG6PT infusion increased bone marrow cellularity and the total cell numbers in the infused G6PT$^{-/-}$ mice at 2 weeks of age increased to 57% of the control G6PT$^{+/+}$ littermates (Figure 6a). The total numbers of cells in the spleen in 2-week-old G6PT$^{-/-}$ mice were 35% of those in G6PT$^{+/+}$ littermates (Figure 6b). Again, Ad-hG6PT infusion increased the growth of spleen in G6PT$^{-/-}$ mice and the cell numbers increased to 81% of the G6PT$^{+/+}$ littermates at 2 weeks post-infusion (Figure 6b).

The G6PT$^{-/-}$ bone marrow and spleen have a marked increase in colony-forming progenitor cells, which may compensate for the hypocellularity in these tissues.[12] The bone marrow aspirates, combined from the femur, tibia and spleen, in 2-week-old G6PT$^{-/-}$ mice contained a higher proportion of colony forming units (CFU) than the G6PT$^{+/+}$ mice (Figure 6). *In vitro* clonal stimulation of G6PT$^{-/-}$ bone marrow aspirates with G-CSF, granulocyte macrophage-CSF (GM-CSF), or macrophage-CSF (M-CSF) revealed 5.8-fold more CFU-G, 5.2-fold more CFU-GM, and 3.8-fold more CFU-M than produced by the G6PT$^{+/+}$ littermates (Figure 6a). This increase in CFU was normalized by Ad-hG6PT infusion (Figure 6a). The numbers of splenic CFU-G, CFU-GM, and CFU-M in 2-week-old G6PT$^{-/-}$ mice were 6.3-, 4.8-, and 5.9-fold higher, respectively than age-matched control mice (Figure 6b), consistent with the bone marrow aspirates. Again, Ad-hG6PT infusion normalized the increase in spleen CFUs (Figure 6b).

Ad-hG6PT-infusion of 2-week-old G6PT$^{-/-}$ mice corrects metabolic and myeloid dysfunctions in GSD-Ib

Because fetal liver is a hematopoietic organ in the first 10 postnatal days of life[15], we conducted additional studies using older G6PT$^{-/-}$ mice to ensure that Ad-hG6PT-mediated gene transfer delivered the transgene to gluconeogenic as well as myeloid tissues. Two-week-old G6PT$^{-/-}$ mice were infused intravenously with 3×10^8 PFU of Ad-hG6PT, and hG6PT transcripts in the liver, kidney, bone marrow, and spleen were quantified 1 week post-infusion; the expression levels were normalized to the level of G6PT transcript in the transduced liver. Again, Ad-hG6PT efficiently delivered the transgene to the liver (100%), bone marrow (4.2 %), and spleen (20.4%) (Figure 1b). However, the transgene was not delivered efficiently to the kidney (1.6%) of G6PT$^{-/-}$ mice (Figure 1a). Hepatic microsomal G6P transport activity in the infused G6PT$^{-/-}$ mice at 3 weeks of age (1-week post-infusion) was 54% of the activity in hepatic microsomes of age-matched G6PT$^{+/+}$ littermates (Figure 7a). As expected the infused G6PT$^{-/-}$ mice exhibit improved growth, normalized plasma glucose, cholesterol, triglyceride,

uric acid, and lactic acid levels, and reduced hepatic glycogen storage and hepatomegaly (data not shown).

Delivery of the G6PT gene into the bone marrow and spleen of 2-week-old G6PT$^{-/-}$ mice also improved myeloid functions. Neutrophil counts are severely depressed in 3-week-old G6PT$^{-/-}$ mice with counts of 195 ± 18/μl, compared to 1362 ± 128/μl in wild-type littermates. The infused G6PT$^{-/-}$ mice at 3 weeks of age exhibited improved neutropenia with neutrophil counts increased to 967 ± 147/μl (Figure 7b). Infusion of 2-week-old G6PT$^{-/-}$ mice with Ad-hG6PT also corrected the abnormal elevation in serum G-CSF levels (Figure 7c), increased cellularity in the bone marrow (Figure 7d), and normalized myeloid progenitor cells frequencies in the bone marrow (Figure 7d) and the spleen (Figure 7e). However, at one week post-Ad-G6PT infusion the spleen cell counts were not significantly increased in the infused G6PT$^{-/-}$ mice (Figure 7e). The lack of correction in spleen growth may result from the short duration (1 week) of the Ad-hG6PT-meidated gene therapy.

Discussion

G6PT is a ubiquitously expressed[3], highly hydrophobic, transmembrane ER protein[11] which can not be expressed in a soluble form. To be effect, G6PT must embed within the ER membrane in the correct conformation to not only transport G6P but also couple functionally to the hydrolytic enzyme glucose-6-phosphatase-α.[16,17] Failure to achieve both of these goals results in an ineffective G6Pase system. In the gluconeogenic tissue - the liver, the kidney and the intestine - this failure results in fasting hypoglycemia, hepatomegaly, nephromegaly, hyperlipidemia, hyperuricemia, lactic academia, and growth retardation.[1,2] An additional complication of GSD-Ib is myeloid dysfunction. Our hypothesis proposes that to correct this symptom, G6PT activity must also be restored in the myeloid cell lineages. Therefore, to correct all of the abnormalities associated with GSD-Ib, a functional G6PT must be expressed in multiple tissues. In this study we have evaluated gene replacement therapy for this inheritable disorder using a recombinant adenovirus carrying G6PT. We show that Ad-hG6PT can effectively deliver the G6PT transgene to the liver, bone marrow, and spleen in a way that corrects both the metabolic and myeloid abnormalities in murine GSD-Ib. The GSD-Ib mice receiving the recombinant virus exhibit improved growth; normalized serum profiles of glucose, cholesterol, triglyceride, uric acid and lactate; reduced hepatic glycogen storage; and improved hepatomegaly. These changes are all consistent with the reconstitution of a functional G6Pase system in the gluconeogenic tissues. In addition, the adenoviral-mediated gene transfer also improves neutropenia; normalizes serum G-CSF levels; improves bone and spleen development; leads to increased cellularity of the bone and spleen; and normalizes myeloid progenitor cell frequencies in both tissues. These findings are consistent with the reconstitution of G6PT activity in the myeloid cells.

In contrast to the G6PT reconstitution within the liver, bone marrow, and spleen, effective adenovirus-mediated G6PT transduction of the kidney does not occur, and typical GSD-Ib characteristics of kidney enlargement associated with abnormal glycogen deposition, continues to develop. Therefore, correction of the full phenotype of GSD-Ib will require co-transfection of an adenoviral vector carrying G6PT with a second G6PT carrying vector capable of transducing the kidney, or the use of a single vector with a liver, kidney, bone marrow and spleen transduction potential.

To date, seven human GSD-Ib patients have received orthotopic liver transplantation and all showed improved metabolic profiles following transplantation.[18-22] This is consistent with our findings, which also suggest the kidney has a secondary role in glucose homeostasis relative to the liver because the liver G6PT transduction alone corrected the metabolic abnormalities in GSD-Ib mice. Our findings also suggest that reconstitution of a functional liver G6PT is not

sufficient to prevent metabolic consequences in the kidney. There is little human patient data on this issue. Renal function was examined in only one of the liver transplantation patients above, however in that single case the kidney remained normal 6.2 years after transplantation.[19] The role of liver transplantation in preventing renal complications in humans remains unclear. Our findings do, however, clearly dissociate the expression of G6PT in the kidney from the myeloid dysfunctions.

Of the currently available viral vectors, adenovirus[23] and adeno-associated virus (AAV)[24] are two of the most efficient at transducing nondividing cells and both have the potential to transduce a variety of different tissues including liver, skeletal muscle, and lung. *In vitro* studies had suggested the adenoviral vectors might be effective with bone marrow cells[25] and embryonic stem cells[26] and the AAV serotype 1[27] might be effective with primitive murine hematopoietic stem cells. Until this study, there has been no information on the ability of recombinant adenovirus or AAV to deliver a transgene to myeloid tissues *in vivo*. Our finding that intravenous infusion of a recombinant adenovirus can deliver a functional transgene to both the bone marrow and spleen, may prove of value in other fields. The adenoviral vector used in this study is limited by the short-term expression of the transgene.[28,29] and effective gene therapy requires sustained expression of the transgene. Helper-dependent adenoviral vectors deleting most or all of the viral protein encoding sequence which are significantly less toxic are now available.[30,31] and may be more attractive in the future. Also, AAV vectors are not considered pathogenic and have not been implicated in known human diseases[32,33] Therefore, further investigation is required to identify a more comprehensive gene therapy vector that will achieve long-term correction of metabolic and myeloid dysfunctions in GSD-Ib or that a transgene can be repeatedly administrated in the absence of adverse immune responses.

In summary, using a murine model of GSD-Ib, we have demonstrated that an adenovirus-mediated gene therapy can deliver the G6PT transgene to multiple tissues including the liver, bone marrow and spleen, correcting both the metabolic and myeloid dysfunctions in GSD-Ib. Our study suggests that human GSD-Ib may be amenable to G6PT gene therapy when the G6PT transgene expression can be sustained and that the adenoviral-based gene therapy approach may be relevant to *in vivo* studies of bone marrow and spleen function.

Materials and methods

Infusion of G6PT$^{-/-}$ mice with Ad-hG6PT

A human G6PT-bearing E1- and E3-deleted adenovirus (Ad-hG6PT) was generated by the Cre-*lox* recombination system as previously described.[34] Ad-hG6PT was grown and purified by CsCl density ultracentrifugation and quantified by plaque assays. All animal studies were conducted under an animal protocol approved by the NICHD Animal Care and Use Committee. A glucose therapy that is comprised of intra-peritoneal or subcutaneous injection of 25 to 100 μl of 15% glucose every 12 h starting at the first post-natal day was administered to the G6PT$^{-/-}$ mice as described previously.[12] Mice that survived weaning were given unrestricted access to Mouse Chow (Zeigler Bros., Inc., Gardners, PA). GSD-Ib is an autosomal recessive disorder.[1,2] Since the phenotypes of G6PT$^{+/+}$ and G6PT$^{+/-}$ mice are identical, and both exhibit normal development, metabolic functions and myeloid functions[12], we will use the designation G6PT$^{+/+}$ mice to refer to the wild type phenotype represented by G6PT$^{+/+}$ or G6PT$^{+/-}$ mice.

Fetal liver is a hematopoietic organ in the first 10 postnatal days[15]; therefore, we conducted two parallel studies to ensure that Ad-hG6PT-mediated gene transfer delivered the transgene to gluconeogenic as well as myeloid tissues. One group of mice was infused neonatally, the second group was infused when the animals reached age 2 weeks.

Neonatal (1 or 2-day-old) G6PT$^{-/-}$ mice were infused via the temporal vein with 30 μl of Ad-hG6PT containing 5×10^7 PFU and 2-week-old G6PT$^{-/-}$ mice were infused via the retro-orbital vein with 100 μl of Ad-hG6PT containing 3×10^8 PFU. Glucose therapy was terminated immediately in Ad-hG6PT-infused G6PT$^{-/-}$ mice and the weaning mice were given Mouse Chow *ad libitum*.

Real-time RT-PCR Analysis

Total RNAs were isolated from wild-type and Ad-hG6PT-infused mouse tissues using TRIzol Reagent (Invitrogen Life Technologies, Carlsbad, CA). The G6PT transcripts were quantified by real-time RT-PCR, in triplicate, in an Applied Biosystems 7300 Real-Time PCR System (Applied Biosystems, Foster City, CA, USA) using the gene-specific TaqMan® Gene Expression Assays and then normalized to GAPDH RNA. The human G6PT probe (Applied Biosystems Assay ID Hs 00184616_m1) will generate an amplicon of 88 bases containing nucleotides 774 to 861 (NM_001467) of the human G6PT transcript and the mouse G6PT probe (Applied Biosystems Assay ID Mm 00484574_m1) will generate an amplicon of 56 bases containing nucleotides 418 to 473(NM_008063) of the mouse G6PT transcript. Data were analyzed using the SDS v1.3 software (Applied Biosystems) and expression levels normalized by the level of G6PT transcript in the liver.

G6P uptake assays

Microsomal preparations and G6P uptake measurement were performed as described previously.[17] Briefly, microsomes were incubated in a reaction mixture (100 μl) containing 50 mM sodium cacodylate buffer pH 6.5, 250 mM sucrose, and 0.2 mM [U-^{14}C]G6P (50 μCi/μmol). The reaction was stopped at the appropriate time by filtering immediately through a nitrocellulose membrane (BA85, Schleicher & Schuell, Keene, NH). Since an enzymatically active G6Pase-α is located in the microsomes, the [U-^{14}C]G6P taken up by the microsomes is hydrolyzed to [U-^{14}C]glucose. Thus, the radioactive molecules accumulated inside the microsomes include both [U-^{14}C]G6P and [U-^{14}C]glucose. Microsomes permeabilized with 0.2% deoxycholate, to abolish G6P uptake, were used as negative controls.

Hematological and phenotype Analyses

Blood samples were collected from the tail vein using EDTA-containing CAPIJECT tubes (TerumoMedical Co., Elkton, MD) for the differential leukocyte counts. Manual 200-cell leukocyte differential counts of peripheral blood cells were performed on Hema 3 (Fisher Scientific, Pittsburgh, PA.) stained smears. Bone marrow cells from femoral and tibia bones were harvested by flushing with 3 ml of Iscove's modified Dulbecco's medium containing 2% fetal bovine serum.

Serum glucose, total cholesterol, and uric acid were analyzed using kits obtained from Thermo Electron (Louisville, CO). Triglycerides were measured with a kit from Sigma Diagnostics (St Louis, MO) and lactate measured by a kit from Trinity Biotech (St. Louis, MO). G-CSF was quantified using Quantikine ELISA kits (R&D Systems Inc., Minneapolis, MN).

For H&E staining, tissues were preserved in 10% neutral buffered formalin, embedded in paraffin, and sectioned at 4-6 microns thickness.

Hematopoietic Progenitor Cell Assays

Progenitor cells were assayed in semisolid agar cultures by plating 2×10^4 bone marrow or 10^5 spleen cells in 1 ml of methylcellulose media (MethoCult M3231, Stem Cell Technologies, Vancouver, Canada) supplemented with the indicated cytokines. The number of colonies larger

than 50 cells was counted on days 7 to 9. Recombinant murine cytokines (R&D Systems) used were: G-CSF (10 ng/ml), GM-CSF (10 ng/ml), or M-CSF (2.5 ng/ml).

Statistical Analysis

Statistical analysis using the unpaired t test was performed with The GraphPad Prism Program (GraphPad Software, San Diego, CA). Values were considered statistically significant at $p < 0.05$.

Acknowledgement

We thank Dr. Brian C Mansfield for critical reading of the manuscript.

References

1. Chou JY, Matern D, Mansfield BC, Chen YT. Type I glycogen storage diseases: disorders of the glucose-6-phosphatase complex. Curr Mol Med 2002;2:121–143. [PubMed: 11949931]
2. Chen, Y-T. Glycogen storage diseases. In: Scriver, CR.; Beaudet, AL.; Sly, WS.; Valle, D.; Childs, B.; Kinzler, KW.; Vogelstein, B., editors. The Metabolic and Molecular Bases of Inherited Disease. 8th edn.. McGraw-Hill Inc.; New York: 2001. p. 1521-1551.
3. Lin B, Annabi B, Hiraiwa H, Pan C-J, Chou JY. Cloning and characterization of cDNAs encoding a candidate glycogen storage disease type 1b protein in rodents. J Biol Chem 1998;273:31656–31670. [PubMed: 9822626]
4. Gitzelmann R, Bosshard NU. Defective neutrophil and monocyte functions in glycogen storage disease type 1b: a literature review. Eur J Pediatr 1993;152:S33–S38. [PubMed: 8391445]
5. Garty B, Douglas S, Danon YL. Immune deficiency in glycogen storage disease type 1b. Isr J Med Sci 1996;32:1276–1281. [PubMed: 9007171]
6. Chou, JY.; Mansfield, BC. Glucose-6-phosphate transporter: the key to glycogen storage disease type Ib. In: Broer, S.; Wagner, CA., editors. Membrane Transporter Diseases. Kluwe Academic/Plenum Publishers; New York: 2003. 2003. p. 191-205.
7. Greene HL, Slonim AE, O'Neill JA Jr, Burr IM. Continuous nocturnal intragastric feeding for management of type 1 glycogen-storage disease. N Engl J Med 1976;294:423–425. [PubMed: 813144]
8. Chen YT, Cornblath M, Sidbury JB. Cornstarch therapy in type I glycogen storage disease. N Engl J Med 1984;310:171–175. [PubMed: 6581385]
9. Schroten H, Roesler J, Breidenbach T, Wendel U, Elsner J, Schweitzer S, et al. Granulocyte and granulocyte-macrophage colony-stimulating factors for treatment of neutropenia in glycogen storage disease type Ib. J Pediatr 1991;119:748–754. [PubMed: 1719175]
10. Roe TF, Coates TD, Thomas DW, Miller JH, Gilsanz V. Brief report: treatment of chronic inflammatory bowel disease in glycogen storage disease type Ib with colony-stimulating factors. N Engl J Med 1992;326:1666–1669. [PubMed: 1375344]
11. Pan C-J, Lin B, Chou JY. Transmembrane topology of human Glucose-6-phosphate transporter. J Biol Chem 1999;274:13865–13869. [PubMed: 10318794]
12. Chen L-Y, Shieh J-J, Lin B, Pan C-J, Gao J-L, Murphy PM, et al. Impaired glucose homeostasis, neutrophil rafficking and function in mice lacking the glucose-6-phosphate transporter. Hum Mol Genet 2003;12:2547–2558. [PubMed: 12925567]
13. Pan C-J, Kei K-J, Chen H, Ward JM, Chou JY. Ontogeny of the murine glucose-6-phosphatase system. Arch Biochem Biophys 1998;358:17–24. [PubMed: 9750160]
14. Sieff, CA.; Nathan, DG.; Clark, SC. The anatomy and physiology of hematopoiesis. In: Nathon, DG.; Orkin, SH., editors. Hematology of Infancy and Childhood. 5th edn.. 1. WB Saunders; Philadelphia: 1998. p. 161-236.
15. Wolber FM, Leonard E, Michael S, Orschell-Traycoff CM, Yoder MC, Srour EF. Roles of spleen and liver in development of the murine hematopoietic system. Exp Hematol 2002;30:010–1019.
16. Lei K-J, Chen H, Pan C-J, Ward JM, Mosinger B, Lee EJ, et al. Glucose-6-phosphatase dependent substrate transport in the glycogen storage disease type 1a mouse. Nat Genet 1996;13:203–209. [PubMed: 8640227]

17. Hiraiwa H, Pan C-J, Lin B, Moses SW, Chou JY. Inactivation of the glucose-6-phosphate transporter causes glycogen storage disease type 1b. J Biol Chem 1999;274:5532–5536. [PubMed: 10026167]

18. Lachaux A, Boillot O, Stamm D, Canterino I, Dumontet C, Regnier F, et al. Treatment with lenograstim (glycosylated recombinant human granulocyte colony-stimulating factor) and orthotopic liver transplantation for glycogen storage disease type Ib. J. Pediatr 1993;123:1005–1008. [PubMed: 7693904]

19. Matern D, Starzl TE, Arnaout W, Barnard J, Bynon JS, Dhawan A, et al. Liver transplantation for glycogen storage disease types I, III, and IV. Eur J Pediatr 1999;158:S43–S48. [PubMed: 10603098]

20. Martinez-Olmos MA, Lopez-Sanroman A, Martin-Vaquero P, Molina-Perez E, Barcena R, Vicente E, et al. Liver transplantation for type Ib glycogenosis with reversal of cyclic neutropenia. Clin Nutr 2001;20:375–377. [PubMed: 11478837]

21. Bhattacharya K, Heaton N, Rela M, Walter JH, Lee PJ. The benefits of liver transplantation in glycogenosis type Ib. J Inherit Metab Dis 2004;27:539–540. [PubMed: 15334736]

22. Adachi M, Shinkai M, Ohhama Y, Tachibana K, Kuratsuji T, Saji H, et al. Improved neutrophil function in a glycogen storage disease type 1b patient after liver transplantation. Eur J Pediatr 2004;163:202–206. [PubMed: 14872340]

23. Breyer B, Jiang W, Cheng H, Zhou L, Paul R, Feng T, et al. Adenoviral vector-mediated gene transfer for human gene therapy. Curr Gene Ther 2001;1:149–162. [PubMed: 12108952]

24. Carter PJ, Samulski RJ. Adeno-associated viral vectors as gene delivery vehicles. Int J Mol Med 2000;6:17–27. [PubMed: 10851261]

25. Mitani K, Graham FL, Caskey CT. Transduction of human bone marrow by adenoviral vector. Hum Gene Ther 1994;5:941–948. [PubMed: 7948143]

26. Mitani K, Wakamiya M, Hasty P, Graham FL, Bradley A, Caskey CT. Gene targeting in mouse embryonic stem cells with an adenoviral vector. Somat Cell Mol Genet 1995;21:221–231. [PubMed: 8525428]

27. Zhong L, Li W, Li Y, Zhao W, Wu J, Li B, et al. Evaluation of primitive murine hematopoietic stem and progenitor cell transduction in vitro and in vivo by recombinant adeno-associated virus vector serotypes 1 through 5. Hum Gene Ther 2006;17:321–333. [PubMed: 16544981]

28. Benihoud K, Yeh P, Perricaudet M. Adenovirus vectors for gene delivery. Curr Opin Biotechnol 1999;10:440–447. [PubMed: 10508634]

29. Wilson JM. Adenovirus-mediated gene transfer to liver. Adv Drug Deliv Rev 2001;46:205–209. [PubMed: 11259841]

30. Palmer DJ, Ng P. Helper-dependent adenoviral vectors for gene therapy. Hum Gene Ther 2005;16:1–16. [PubMed: 15703484]

31. Alba R, Bosch A, Chillon M. Gutless adenovirus: last-generation adenovirus for gene therapy. Gene Ther 2005;12(Suppl 1):S18–S27. [PubMed: 16231052]

32. Tenenbaum L, Lehtonen E, Monahan PE. Evaluation of risks related to the use of adeno-associated virus-based vectors. Curr Gene Ther 2003;3:545–565. [PubMed: 14683451]

33. Flotte TR. Gene therapy progress and prospects: recombinant adeno-associated virus (rAAV) vectors. Gene Ther 2004;11:805–810. [PubMed: 15042119]

34. Chen L-Y, Pan C-J, Shieh J-J, Chou JY. Structure-function analysis of the glucose-6-phosphate transporter deficient in glycogen storage disease type Ib. Hum Mol Genet 2002;11:3199–3207. [PubMed: 12444104]

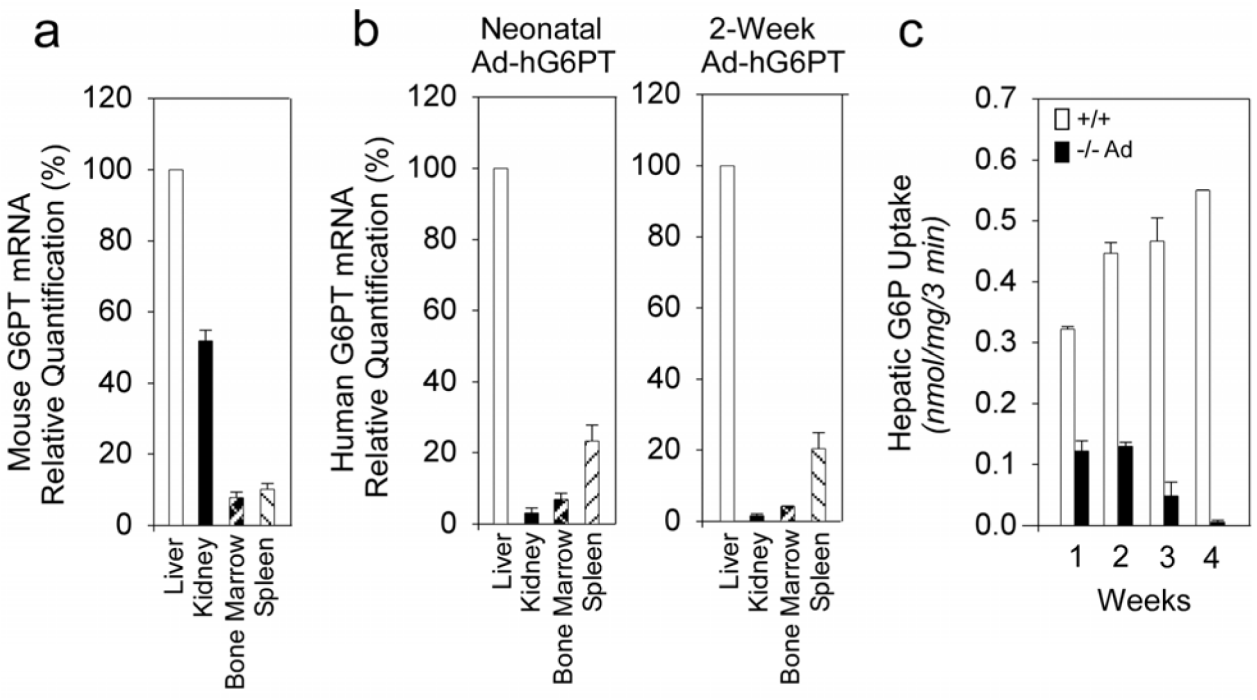

Figure 1.

G6PT mRNA expression and microsomal G6P uptake activity. (a) Quantification of mouse G6PT mRNA in 2- to 3-week-old wild-type mice by real-time PCR. The expression levels were normalized by the level of G6PT transcript in the liver, values at 100%. (b) Quantification of human G6PT mRNA by real-time PCR. Human G6PT transcript was examined in neonatally Ad-hG6PT-infused G6PT$^{-/-}$ mice at 2 weeks post-infusion and in postnatally (2-week-old) Ad-hG6PT-infused G6PT$^{-/-}$ mice at 1 week post-infusion. The expression levels were normalized by the level of human G6PT transcript in the infused liver, values at 100%. (b) Hepatic microsomal G6P uptake activities in the infused G6PT$^{-/-}$ (-/- Ad) and age-matched G6PT$^{+/+}$ (+/+) mice. Values reported have been corrected for background by subtracting hepatic microsomal G6P uptake activity (0.013 ± 0.002 *nmol/mg/3 min*) in the untreated G6PT$^{-/-}$ mice. Data are presented as the mean ± SEM.

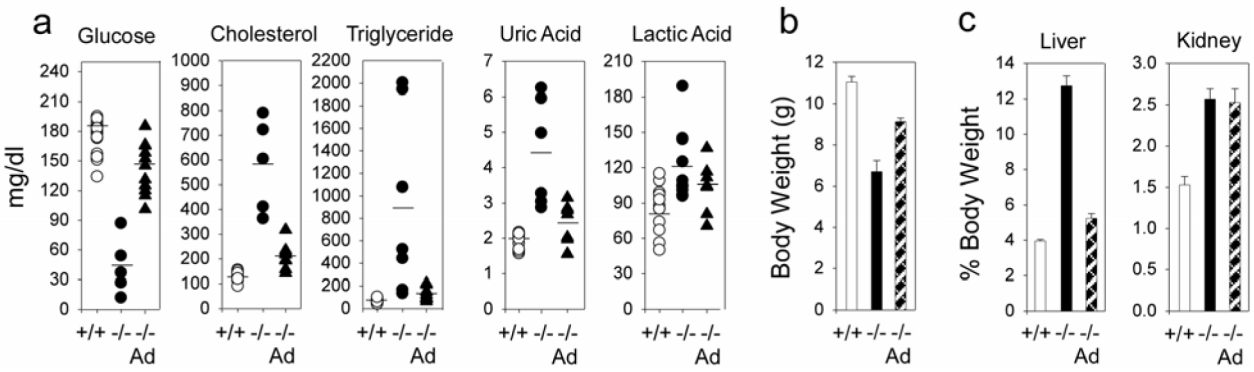

Figure 2.

Analyses of metabolic functions after neonatal infusion of G6PT$^{-/-}$ mice with Ad-hG6PT. Metabolic functions were analyzed in the Ad-hG6PT-infused G6PT$^{-/-}$ mice (-/- Ad) at 2 weeks post-infusion. Age-matched G6PT$^{+/+}$ (+/+) and G6PT$^{-/-}$ (-/-) mice were used as controls. The unpaired *t* test was used to evaluate the statistical difference between +/+ & -/- mice and between -/- Ad & -/- mice. (a) Serum glucose, cholesterol, triglyceride, uric acid, and lactic acid levels. Horizontal bars indicate the mean concentrations. (b) Body weight. Data are presented as mean ± SEM. $p < 0.0001$ for both comparisons. (c) The weights of the liver and kidney relative to total body weight. Liver weights, $p < 0.0001$ for both comparisons. Kidney weight, $p < 0.0001$ for +/+ & -/- comparison and the difference between -/- Ad & -/- is not statistically significant.

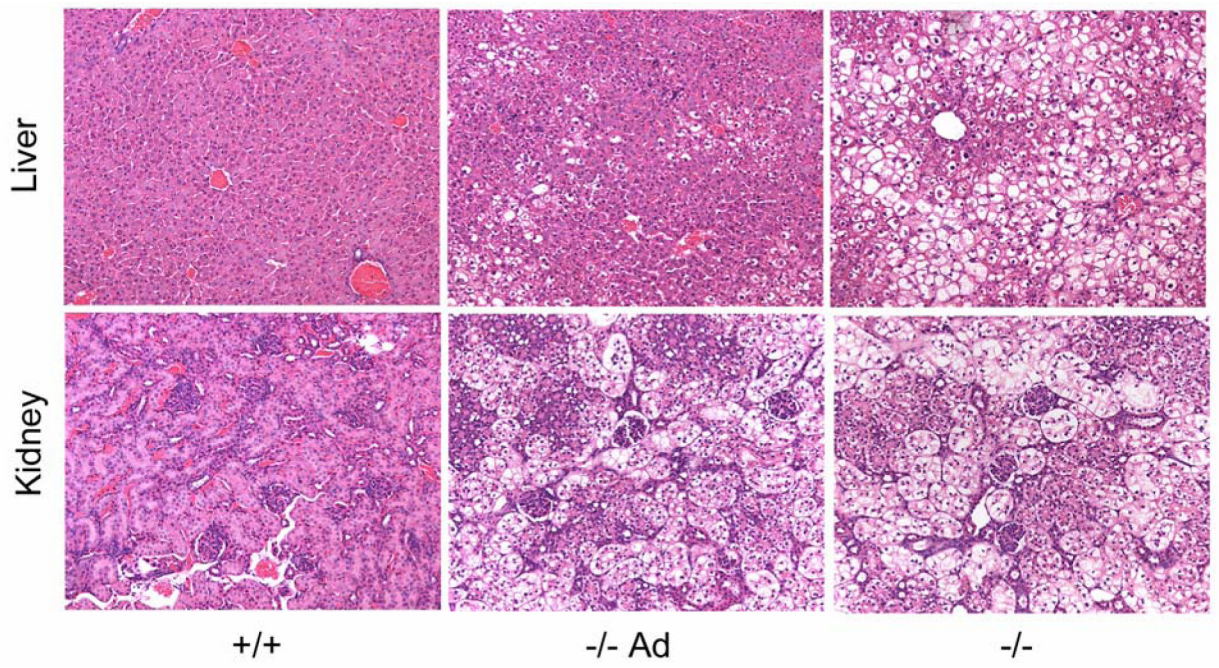

Figure 3.

Histological analysis of the liver and kidney from the Ad-hG6PT-infused newborn G6PT$^{-/-}$ mice. Plates show hematoxylin-eosin stained liver and kidney sections from G6PT$^{+/+}$ (+/+), Ad-hG6PT-infused G6PT$^{-/-}$ (-/- Ad), and untreated G6PT$^{-/-}$ (-/-) mice at 2 weeks postinfusion with magnifications of ×200.

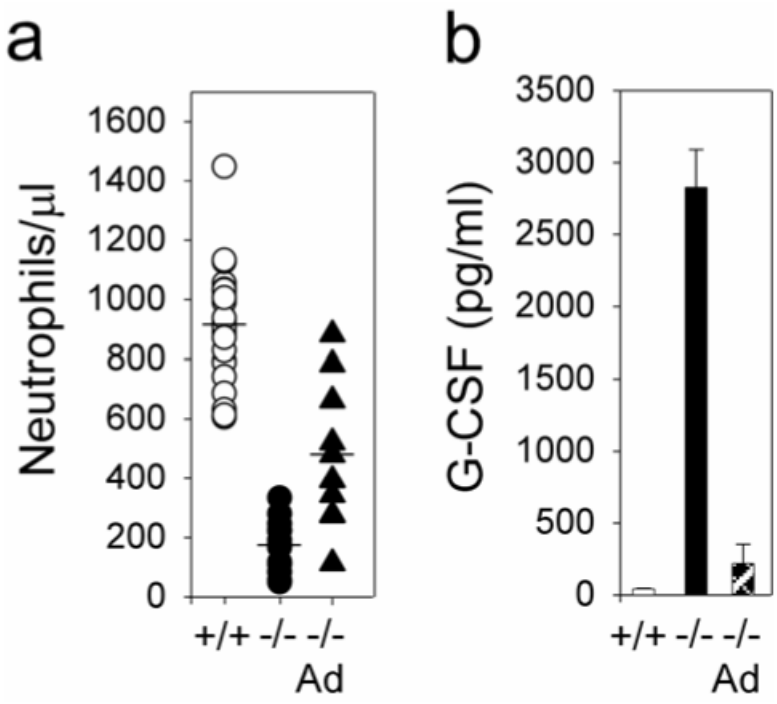

Figure 4.

Neutrophil counts and serum G-CSF levels after neonatal infusion of G6PT$^{-/-}$ mice with Ad-hG6PT. Myeloid functions were analyzed in the Ad-hG6PT-infused G6PT$^{-/-}$ mice (-/- Ad) at 2 weeks post-infusion. Age-matched G6PT$^{+/+}$ (+/+) and G6PT$^{-/-}$ (-/-) mice were used as controls. The unpaired *t* test was used to evaluate the statistical difference between +/+ & -/- and between -/- Ad & -/- mice. (a) Blood neutrophil counts. Horizontal bars indicate the mean concentrations. $p < 0.0002$ for both comparisons. (b) Serum G-CSF levels. Data are presented as the means ± SEM. $p < 0.0001$ for both comparisons.

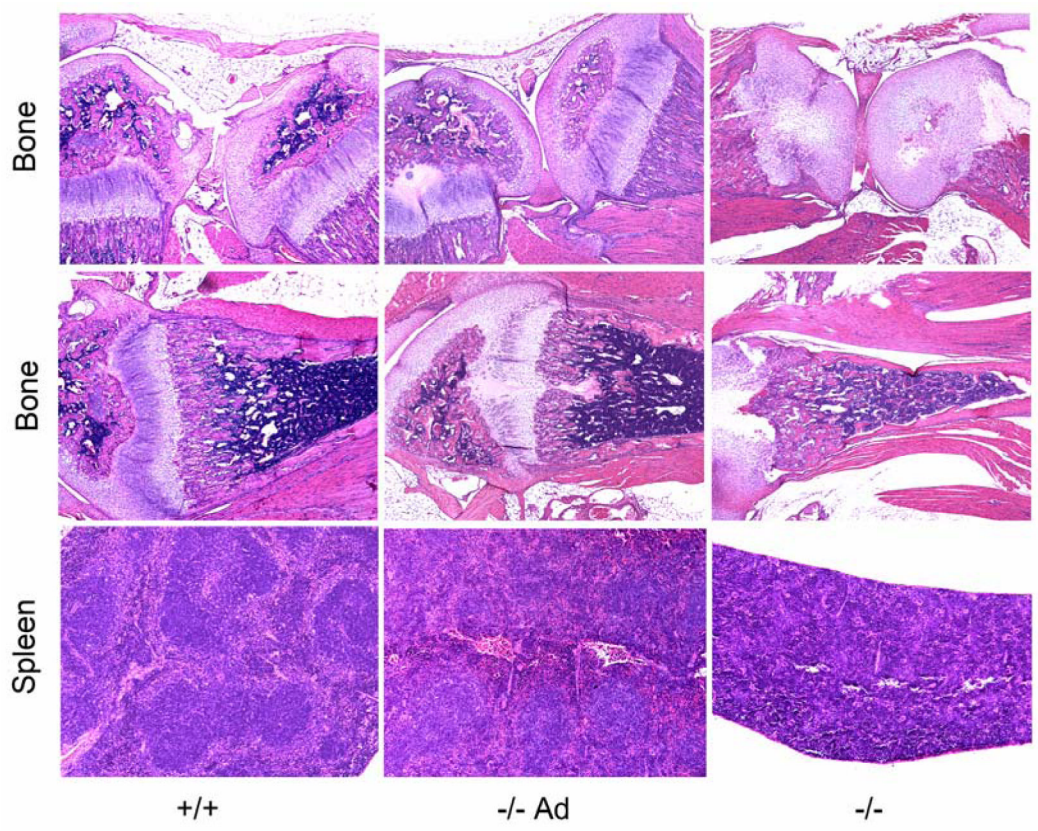

Figure 5.

Histological analyses of bone and spleen. Newborn G6PT$^{-/-}$ mice were infused with Ad-hG6PT (-/- Ad) and bone and spleen were examined at 2 weeks post-infusion. Age-matched G6PT$^{+/+}$ (+/+) and G6PT$^{-/-}$ (-/-) mice were used as controls. H&E stained bone and spleen sections at magnifications of ×50.

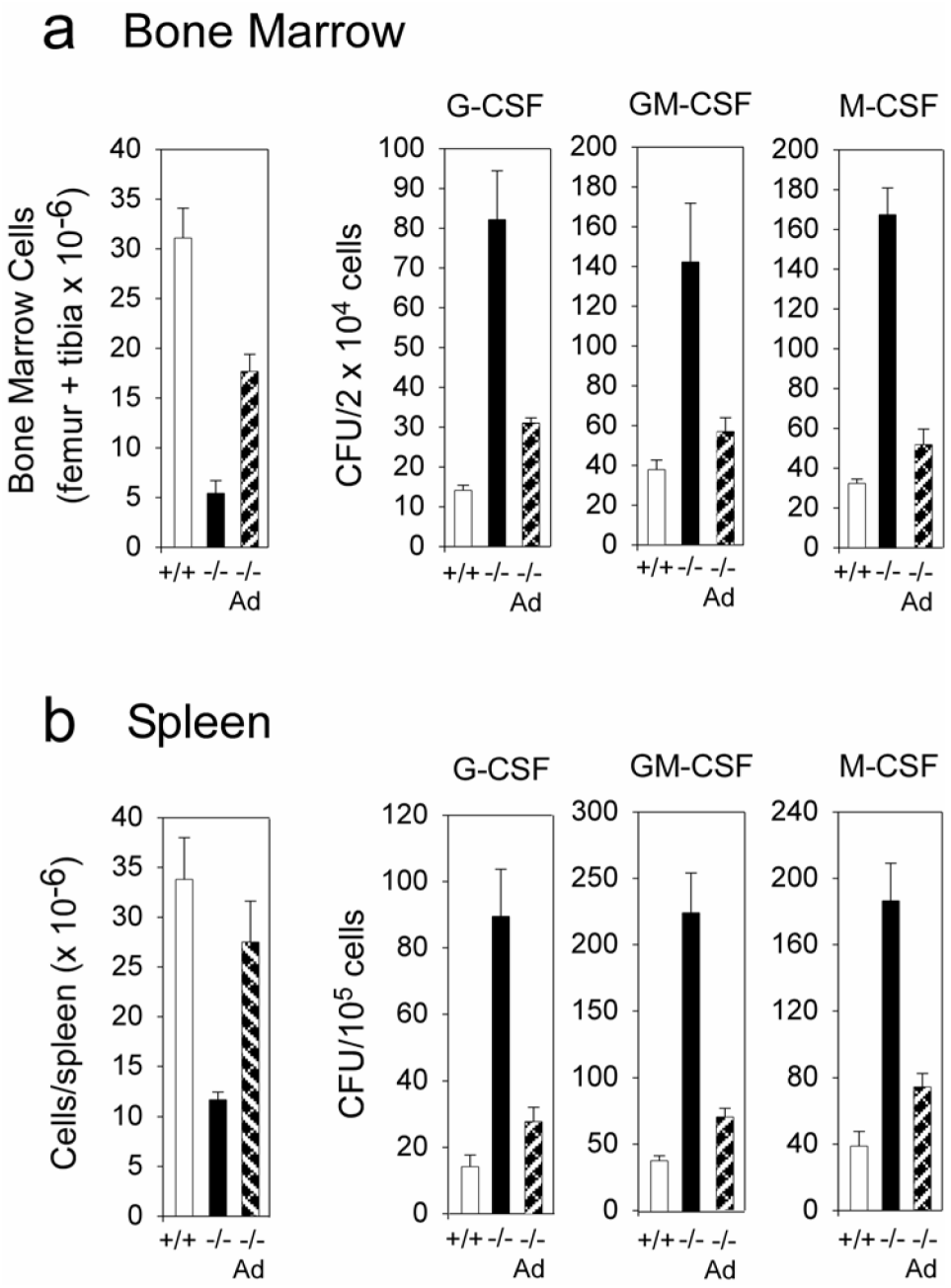

Figure 6.

Total cell counts and myeloid progenitor cells in the femur plus tibia and spleen after neonatal infusion of G6PT$^{-/-}$ mice with Ad-hG6PT. The myeloid functions were were examined at 2 weeks post-infusion in the Ad-hG6PT-infused G6PT$^{-/-}$ mice (-/- Ad). Age-matched G6PT$^{+/+}$ (+/+) and G6PT$^{-/-}$ (-/-) mice were used as controls. CFU were determined following stimulation bone marrow or spleen cells with G-CSF, GM-CSF, or M-CSF. Results are the mean ± SEM from four separate experiments in which each mouse was assessed individually. The unpaired *t* test was used to evaluate the statistical difference between +/+ & -/- and between -/- Ad & -/- mice. (a) Bone marrow. $p < 0.002$ for all comparisons between +/+ & -/- mice; and $p < 0.03$ for all comparisons between -/- Ad & -/- mice. (b) Spleen. $p < 0.001$ for all comparisons between +/+ & -/- mice; and $p < 0.04$ for all comparisons between -/- Ad & -/- mice.

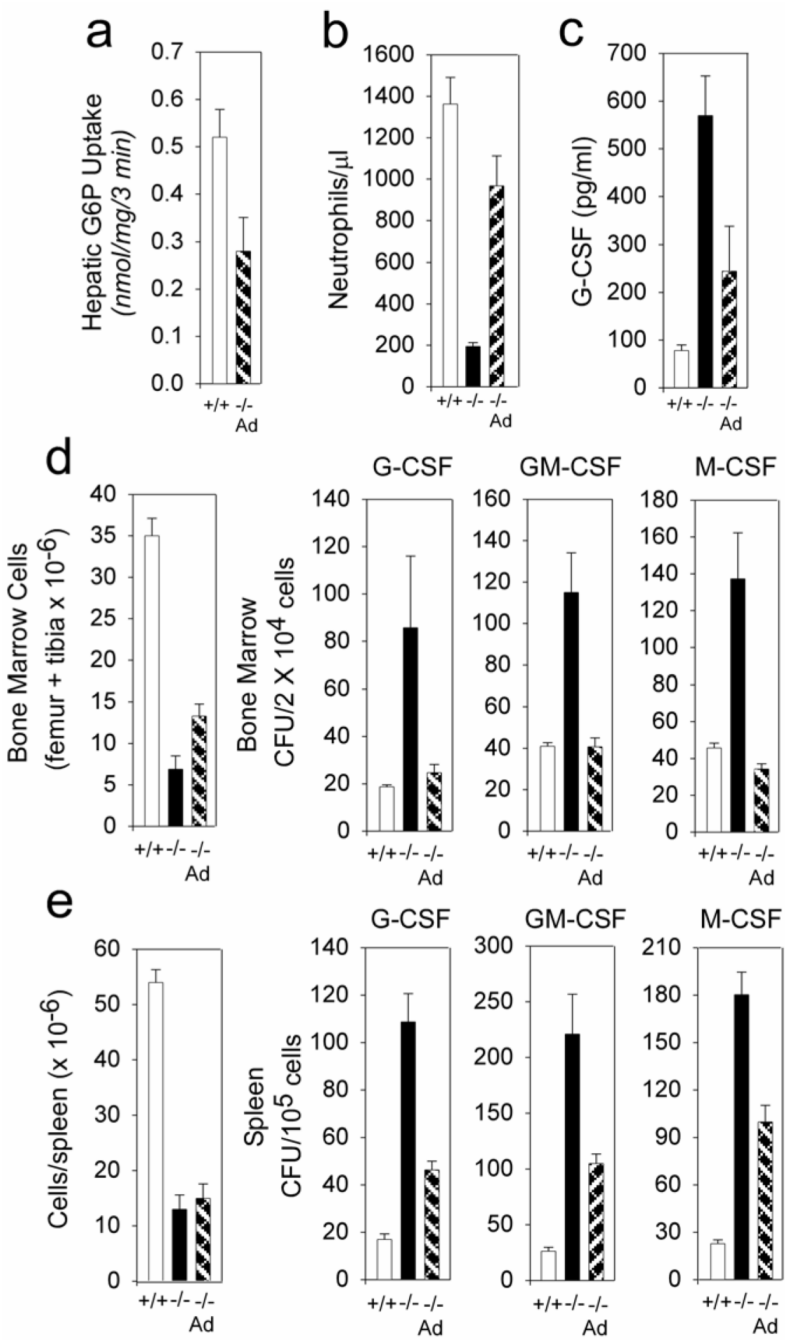

Figure 7.

Microsomal G6P transport activity and myeloid functions following infusion of 2-week-old G6PT$^{-/-}$ mice with Ad-hG6PT. Analyses were performed in the Ad-hG6PT-infused G6PT$^{-/-}$ mice (-/- Ad) when they are 3 week-old (1 week post-infusion). Age-matched G6PT$^{+/+}$ (+/+) and G6PT$^{-/-}$ (-/-) mice were used as controls. Data are presented as the mean ± SEM. The unpaired *t* test was used to evaluate the statistical difference between +/+ & -/- and between -/- Ad & -/- mice. (a) Hepatic microsomal G6P uptake activities. Values reported have been corrected for background by subtracting hepatic microsomal G6P uptake activity (0.013 ± 0.002 *nmol/mg/3 min*) in the untreated G6PT$^{-/-}$ mice. (b) Blood neutrophil counts. $p < 0.0001$ for both comparisons. (c) Serum G-CSF levels. $p < 0.0001$ for both comparisons. (d) Bone

marrow cellularity and myeloid progenitor cells. $p < 0.05$ for all comparisons. (e) Spleen cell counts and myeloid progenitor cells. Cell counts, $p = 0.0002$ for +/+ & -/- mice and $p = 0.06$ for -/- Ad & -/- mice. Myeloid progenitor cells, $p < 0.05$ for all comparisons.